

Membrane-type resonator as an effective miniaturized tuned vibration mass damper

Cite as: AIP Advances 6, 085212 (2016); <https://doi.org/10.1063/1.4961469>

Submitted: 19 May 2016 • Accepted: 09 August 2016 • Published Online: 17 August 2016

Liang Sun,  Ka Yan Au-Yeung, Min Yang, et al.



View Online



Export Citation



CrossMark

ARTICLES YOU MAY BE INTERESTED IN

Membrane- and plate-type acoustic metamaterials

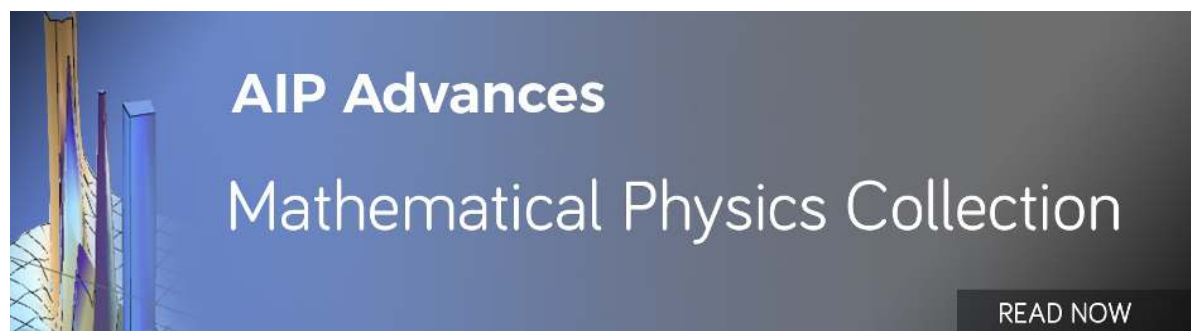
The Journal of the Acoustical Society of America **139**, 3240 (2016); <https://doi.org/10.1121/1.4950751>

Acoustic metamaterial panels for sound attenuation in the 50-1000 Hz regime

Applied Physics Letters **96**, 041906 (2010); <https://doi.org/10.1063/1.3299007>

Acoustic metasurface-based perfect absorber with deep subwavelength thickness

Applied Physics Letters **108**, 063502 (2016); <https://doi.org/10.1063/1.4941338>



AIP Advances
Mathematical Physics Collection

READ NOW

Membrane-type resonator as an effective miniaturized tuned vibration mass damper

Liang Sun, Ka Yan Au-Yeung, Min Yang, Suet To Tang, Zhiyu Yang,^a
and Ping Sheng

*Department of Physics, Hong Kong University of Science and Technology, Clear Water Bay,
Kowloon, Hong Kong, China*

(Received 19 May 2016; accepted 9 August 2016; published online 17 August 2016)

Damping of low frequency vibration by lightweight and compact devices has been a serious challenge in various areas of engineering science. Here we report the experimental realization of a type of miniature low frequency vibration dampers based on decorated membrane resonators. At frequency around 150 Hz, two dampers, each with outer dimensions of 28 mm in diameter and 5 mm in height, and a total mass of 1.78 g which is less than 0.6% of the host structure (a nearly free-standing aluminum beam), can reduce its vibrational amplitude by a factor of 1400, or limit its maximum resonance quality factor to 18. Furthermore, the conceptual design of the dampers lays the foundation and demonstrates the potential of further miniaturization of low frequency dampers. © 2016 Author(s). All article content, except where otherwise noted, is licensed under a Creative Commons Attribution (CC BY) license (<http://creativecommons.org/licenses/by/4.0/>). [<http://dx.doi.org/10.1063/1.4961469>]

Damping of structural vibrations remains a major challenge in many branches of engineering science. Present vibration control technologies can in general be put into three categories, namely passive, active, or semi-active.^{1–3} Due to the performance reliability and maintenance requirements, passive vibration control is often preferred. One of the two most common passive approaches is the surface treatment method^{4,5} with dissipative layer made by high loss factor passive material covering the host structure. However, such methods are limited to high frequencies (usually above 1000 Hz) and add substantial mass load to the host structure. An alternative solution is the tuned mass damper (TMD) with resonances^{6–15} that adds a comparatively lightweight device to the host structure. A typical weight of such a damper for low frequencies in reported experiments is about 10% of the host structure,⁶ and it is usually bulky and requires considerable space.¹³ Other attempts, such as employing poroelastic materials,¹⁶ and introducing nonlinear effects in the tuned mass damper,¹⁷ have been investigated as well. Up to now, it is still particularly challenging to damp low frequency (usually below 500 Hz) vibration and structure borne noise, such as those in aircraft and motor vehicles, by lightweight devices in confined space, as it is still technically very challenging to miniaturize dampers with weight limited to several grams and size limited to centimeters, while still having the low working frequency.

The decorated membrane resonators (DMRs) have been shown as efficient low frequency sound wave shields¹⁸ and absorbers^{19,20} which are light-weight and compact. A theoretical homogenization scheme has been developed to predict the effective parameters and consequently the functionalities of the structures and devices made of multiple DMR's.²¹ More recently, active control by external electric voltage on the properties of DMR's,²² and single incident beam total absorption by combinations of monopole and dipole units have been realized.²³ In this letter, we demonstrate that DMRs can also be effective miniature vibration dampers at low frequency by utilizing the almost divergent effective mass of the DMRs at its “anti-resonance”.¹⁸ By attaching such dampers to the host structure, vibrations at the frequency near the anti-resonance are significantly suppressed. Below, we report the effective implementation of a pair of DMR dampers, each comprising an

^aCorresponding author: email: phyang@ust.hk

elastic membrane fixed on a rigid frame and decorated by a rigid platelet. Suppression of vibrational amplitude of a nearly free-standing aluminum beam by a factor of 1400, or limiting the quality factor (Q-factor) of the beam resonance to 18 or below near 150 Hz were experimentally observed in two types of dampers with different dissipations. Each DMR damper weighs only 1.78 g, or 0.6 % of the aluminum beam, and its low profile and compact outer dimensions are only 28 mm in diameter and 5 mm in height.

For any object with linear internal vibrational degrees of freedom (DOF) that is deep-subwavelength in size, its dynamic effect on a vibrational host body can be fully characterized by the effective mass $m_e \equiv F(\sigma)/\ddot{u}(\sigma) = -F(\sigma)/[\omega^2 u(\sigma)]$ at a location σ on the object (the anchor point) which is in contact with the host body. In the case of a DMR its frame is a natural choice as the anchor point. Here the double-overdot denotes the second derivative respect to time, $\omega = 2\pi f$ is the angular frequency, F is the total external force experienced by the object that is assumed to act only at its anchor, and u is the displacement of the anchor point in real space. With proper internal structures the effective mass of the object could be divergent at selected frequencies, thereby serving as a damper similar to a TMD with multiple DOF.

To understand the presence of divergent effective mass of the damper, we consider a damper with N resonant modes, and notice that its response exhibits the following Lorentzian form:^{20,21}

$$\frac{u(\sigma)}{F(\sigma)} = \sum_{n=1}^N \frac{[u_n(\sigma)]^2}{\rho_n(\omega_n^2 - \omega^2)} + 2i \sum_{n=1}^N \frac{\beta_n [u_n(\sigma)]^2 \omega}{\rho_n(\omega_n^2 - \omega^2)^2}. \quad (1)$$

In Eq. (1), u_n are the eigenmodes under Neumann boundary condition, the displacement-weighted density for the eigenmode u_n of the damper at frequency ω_n is defined as $\rho_n \equiv \int_{\Omega} \rho |u_n|^2 dV$ with ρ being the local mass density and Ω being the volume of the damper. Equation (1) assumes that the dissipation coefficient β_n is small, so that $\omega_n/\beta_n \equiv Q_n \gg 1$. The value of β_n will be determined by fitting to the experiments. For a classic TMD containing a spring joining the oscillator and the anchor base, there are only two resonant modes, the first being the translational motion in free space without distortion of the spring, and the second mode is the relative motion of the base and the oscillator.

Each term in the summation of the real part in Eq. (1) diverges from positive to negative at its resonance frequency. For frequencies between adjacent resonances, contributions from them are usually opposite in sign. Therefore, the so-called ‘‘anti-resonance’’ frequency $\tilde{\omega}$ may exist, at which the responses from the two eigenmodes cancel each other, i.e., $u(\sigma) = 0$ under any force $F(\sigma)$, if the system is without dissipation ($\beta_n = 0$). The associated effective mass thereby diverges. In principle, there could be many anti-resonances, giving rise to multiple band vibration suppression, while for a classic TMD with a single DOF there is only one such frequency. Therefore, a device with properly designed internal structure, even though being compact in size and low in weight, could still act like a TMD with multiple DOF at low frequencies.

To focus on the divergence of mass at a particular low frequency, we consider only the first two lowest resonances in Eq. (1), and further simplify it by treating $\Delta\omega = \tilde{\omega} - \omega$ as a small variable. We denote the derivative of $\text{Re}[u(\sigma)/F(\sigma)]$ with respect to frequency, evaluated at $\tilde{\omega}$, as 2Ξ . By expanding ω around $\tilde{\omega}$ to the first order in $\Delta\omega$, Eq. (1) can be simplified to the form $u(\sigma)/F(\sigma) = 2\Xi(i\beta - \Delta\omega)$, where $\Xi \equiv \sum_{n=1}^2 [u_n(\sigma)]^2 \tilde{\omega} / [\rho_n(\omega_n^2 - \tilde{\omega}^2)^2]$. The effective mass is therefore given by

$$m_e = -\frac{F(\sigma)}{\omega^2 u(\sigma)} = \frac{\Delta\omega + i\beta}{2\Xi\tilde{\omega}^2(\Delta\omega^2 + \beta^2)}. \quad (2)$$

Figure 1(a) shows schematically the structure of the DMR dampers used in the experiments. The elastic membrane (cyan) is 24 mm in diameter, and the circular platelet (gray) is 12 mm in diameter, 1.0 mm in thickness, and weighs 0.54 g. The height of the rigid frame is 5 mm. The mass of the rigid frame is 1.24 g so the total mass of the damper is 1.78 g.

For motions vertical to the membrane plane the lowest frequency eigenmode u_1 of the damper is simply $\omega_1 = 0$ Hz, corresponding to the translational motion without deformation. With membrane tension being 2.633×10^5 Pa, density 1300kg/m^3 , thickness 0.2 mm, and the other dimension

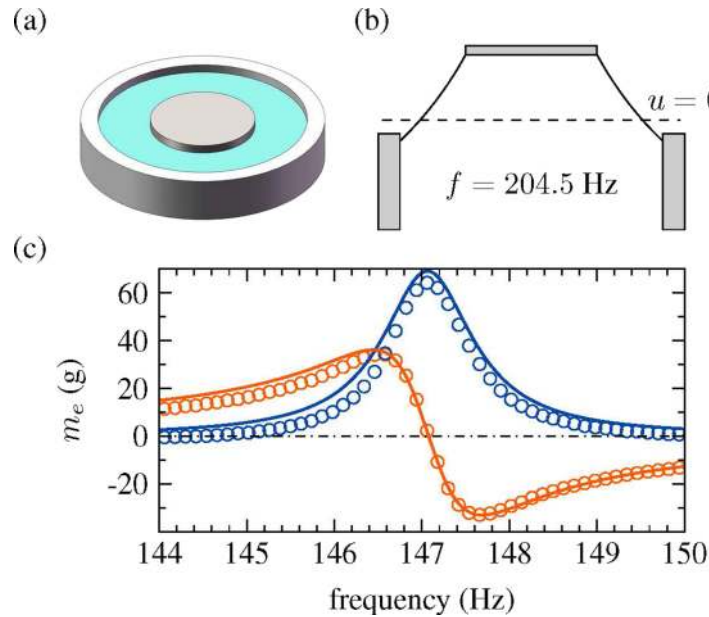


FIG. 1. (a) The schematic illustration of the DMR damper. (b) The first deformed eigenmode of the damper, drawn with axial symmetry assumed. (c) The effective mass of the damper. The real part is shown in orange while the imaginary part is shown in blue. The solid curves are from Eq. (2) and the open circles are from experiments.

parameters given above, theoretical calculations identify the second eigenmode u_2 at 204.5 Hz, at which the central platelet vibrates in the opposite phase to the frame [as shown in Fig. 1(b)]. Anti-resonance with motionless frame occurs at 147.1 Hz due to the interference of the out of phase motion of u_1 and the in-phase motion of u_2 . Based on these two modes, with $\Xi = 2.2 \times 10^{-9} \text{m}^2 \text{s}^3 \text{kg}^{-1}$ and the fitted β being 3.8 Hz, Eq. (2) predicts the effective mass as a function of frequency shown by the curves in Fig. 1(c). This has been confirmed from experiments by mounting the damper on a vibration shaker and recording the relevant acceleration $\ddot{u}(\sigma)$ of the frame and force $F(\sigma)$ acting on the frame by the shaker, and the results are shown by circles in Fig. 1(c). The observed effective mass of the damper reaching 64 g, or ~ 36 times its rest mass around the anti-resonance, indicates a good vibration suppression effect to be expected. Also, near the anti-resonance the damper can be mimicked by a classic TMD with an oscillator mass of 0.54 g, a resonant frequency around 147 Hz, a dashpot that provides a Q-factor around 120, and a base mass of 1.24 g. If such a classic TMD is used to damp the vibration of a host structure, the result is expected to be much the same as that of the DMR damper.

We demonstrate the vibration suppression effects of the DMRs by symmetrically mounting two identical DMR dampers on the ends of a $290 \times 51 \times 4.8$ mm aluminum beam, and exciting the beam at its center with the vibration shaker. The schematic of the setup with the shaker omitted is shown in Fig. 2(a). To tune the first “flapping” resonance mode of the bare beam near the dampers’ anti-resonance at 149 Hz, two extra aluminum blocks with total mass of 97.2 g are added near the beam’s ends, so that the total mass of the bare structure is 288.2 g. At this resonance, the largest motion takes place at the ends of the beam, which is measured by a laser vibrometer and shown as blue circles in Fig. 2(b). At resonance the displacement of the bare beam $|u(\sigma)|$ reaches about 1214 times the amplitude of that of the shaker ξ . The strong vibration is effectively suppressed when the two dampers are mounted. The displacement (orange circles) is drastically reduced to $|u(\sigma)| = 0.813\xi$ at the resonant frequency, which is over 1400 times smaller than that of the bare beam. The total mass of the two dampers is less than 1.2% of that of the host structure.

Similar to a conventional TMD, while the resonant vibration of the host structure near the working frequency $\tilde{\omega}$ of the dampers is suppressed, two new resonances (side bands) located at 140 and 155 Hz are seen to arise below and above $\tilde{\omega}$ as shown in Fig. 2(b). To understand the

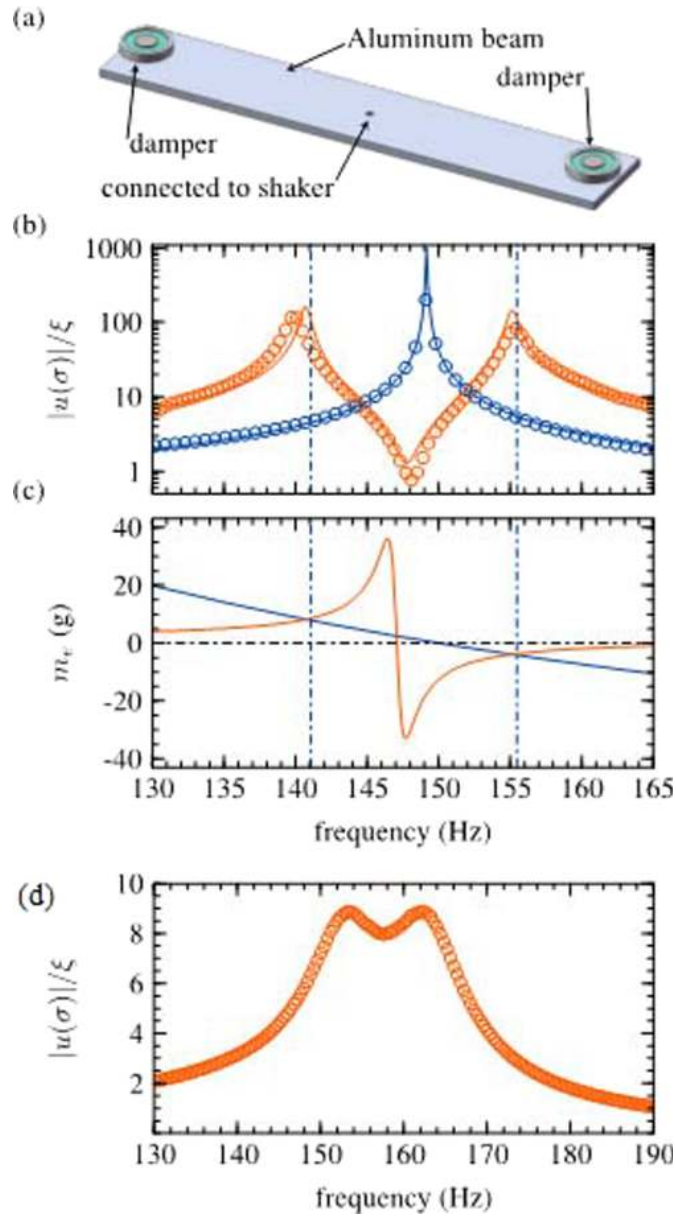


FIG. 2. (a) The schematic illustration of the experimental setups with the shaker omitted due to space limitation. (b) The displacement at the end of the beam $|u(\sigma)|$ normalized by the vibration amplitude of the shaker ξ as a function of frequency. The blue line stands for the case of a bare aluminum beam, and the orange line represents the beam with dampers attached. The solid lines are from Eq. (4) and the open circles are from experiments. (c) The real part of the effective mass for the damper (orange), and the function $1/(\omega^2 G)$ (blue) for the bare beam. Their cross points indicate the emerging of new resonant modes when dampers are attached onto the beam. (d) The displacement at the end of the beam $|u(\sigma)|$ normalized by the amplitude of the shaker ξ as a function of frequency, when two DMR dampers are attached on its two ends by a thin layer of dissipative mud glue.

phenomenon we introduce an analysis in what follows. Denote an operator $P(y, y')$ for the bare beam representing the response displacement at y caused by a displacement excitation at y' , and another operator $G(y, y')$ for the response displacement at y when a force is applied at y' . For the case with dampers on the ends of the beam, $y = \sigma$, the resultant end displacement due to the shaker at $y = 0$ with given displacement ξ is given by

$$u(\sigma) = G(\sigma, \sigma)F(\sigma) + P(\sigma, 0)\xi. \quad (3)$$

Here, F is the force from the damper to the beam, which is $F = \omega^2 m_e u$. Substituting it into Eq. (3), we have

$$u(\sigma) = \frac{P(\sigma, 0)\xi}{1 - \omega^2 m_e G(\sigma, \sigma)}. \quad (4)$$

Equation (4) confirms the vanishing of $u(\sigma)$ when m_e diverges at anti-resonance. Meanwhile, if $1/(\omega^2 G) = m_e$, new resonance emerges with large $u(\sigma)$. We plot $1/(\omega^2 G)$ for the bare beam by the blue line in Fig. 2(c) together with the real part of m_e in orange. Two cross points satisfying the condition $1/(\omega^2 G) = m_e$ can be found that indicate the emergence of new resonances at the frequencies $\omega = 2\pi \times 141.1$ and $2\pi \times 155.5$ Hz, which agree well with the observed resonances. For a given damper, the difference in frequency between the two resonances is determined by the slope of $1/(\omega^2 G)$. Large slope leads to small interval, and vice versa [Fig. 2(c)]. As the response to a force, G is inversely proportional to the mass of the beam. Therefore, if the beam is too heavy, although the suppression effect at anti-resonance still exists, the two new resonances will be too close that make the dip and peaks in Fig. 2(b) undistinguishable from each other. The vibration suppression effect thereby diminishes.

The energy loss in these DMR dampers is small, and its suppression effect is mainly due to the diverged effective mass. In practical applications, dissipation of vibration energy may also be important. The concentration of stress at the interfaces between the dampers and the host structure due to the large effective mass indicates the possibilities of efficient energy absorption by placing a dissipative layer there. In experiment, we use the same dampers as in Fig. 2(a), but add a very thin layer of mud glue (less than 0.2 mm) between the frame of the dampers and the aluminum beam. As shown in Fig. 2(d), although the original dip in the displacement becomes much shallower, the strengths of the two side bands have been greatly reduced. The observed Q-factor for the two peaks is only about 18, which is a significant reduction from that of the bare beam, which is around 1500 as seen in Fig. 2(b).

We now study similar DMR dampers designed to work at an even lower frequency. Circular dampers with larger membrane diameter of 20 mm were fabricated. The diameter of the central platelet is the same as the previous ones, but its mass is almost doubled (~ 0.95 g). The mass of the damper frame is about 1.4 g. The measured effective mass of a typical damper is shown in the insert of Fig. 3. Maximum damping by the damper occurs at 104 Hz. The host structure is a 400 mm \times 400 mm \times 5 mm stainless steel plate with mass of 6.24 kg. It was hanging at the middle point of the top edge by a string and was excited by the shaker at a position about 3 cm above the bottom right corner. The vibration amplitude at the diagonal corner was measured by laser vibrometer. The first resonance of the plate is around 104 Hz. The red curve in Fig. 3

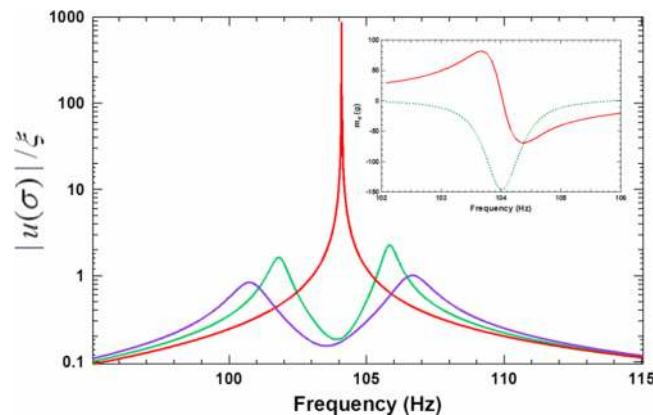


FIG. 3. The displacement at the corner of the plate $|u(\sigma)|$ normalized by the vibration amplitude of the shaker ξ at the diagonal corner as a function of frequency. The red curve is for the plate without dampers. The green and purple curves are for the plate with two and four dampers, respectively. The insert depicts the measured effective mass of a typical damper working at 104 Hz. The red curve represents the real part of the mass, while the green curve represents the imaginary part.

shows the displacement ratio without the dampers. Due to light intrinsic damping, the displacement ratio at resonance exceeded 800, with a Q-factor exceeding 3300. When a damper is placed at each corner next to the excitation corner, the Q-factor of the two split peaks is about 85, and the peak displacement ratio is reduced to 2.3. The minimum displacement ratio is 0.18, a reduction of over 4400 times of the bare plate. When two more dampers are attached to the diagonal corner, the maximum displacement ratio is reduced to 1.0 and the Q-factor is reduced to 42. The total mass of the dampers is about 0.15 % (9.6/6240) of the host structure. From the reduction of Q-factor by two and by four dampers, one could anticipate that the Q-factor would be reduced to 10 if 16 dampers are used. The total weight of the 16 dampers is only about 0.6 % of the host structure.

The design concept of the DMR dampers reported here could serve as the foundation for further development of low frequency miniature dampers. The membrane and the mounting geometry of the platelet form an oscillator with an extremely soft spring, so that even a small oscillator mass around 0.5 g is sufficient to set the working frequency to around 150 Hz. The frequency could be further reduced to around 100 Hz if the mass of the platelet is doubled. The curvature energy¹⁹ provide the dissipation channel so there is no need for a separate dashpot as in the case of classic TMDs. Asymmetric platelets are known for better curvature energy dissipation,¹⁹ so the circular platelet in the present damper is not yet the optimum shape. Energy dissipation can therefore be tuned by changing the shapes of the platelets, without using mud glue for contact which is not easy to control and duplicate. With softer and thinner membranes, even smaller frames and lighter platelets can be used while maintain the working frequency around 100 Hz. Alternatively, with comparable size and mass, an even lower working frequency can be reached. With multiple platelets in each resonator, dampers with multiple working frequency bands can be realized without significant increase in size and weight. The DMR-type devices are therefore promising light-weight miniature low frequency vibration dampers which are well suited for a wide range of applications to eliminate structure borne vibration in light structures with limited available space.

We thank Guancong Ma, Shuyu Chen, Meng Chong, and Binglin Chen for their assistance in some of the experiments. This work is supported by grant ITS/054/12 from the Innovation and Technology Fund of Hong Kong Government.

¹ C. R. Fuller, S. Elliott, and P. A. Nelson, *Active control of vibration* (Academic Press, 1996).

² A. Preumont, *Vibration control of active structures: an introduction* (Springer Science & Business Media, 2012), Vol. 50.

³ D. Karnopp, M. J. Crosby, and R. Harwood, "Vibration control using semi-active force generators," *Journal of Manufacturing Science and Engineering* **96**, 619–626 (1974).

⁴ L. Cremer and M. Heckl, *Structure-borne sound: structural vibrations and sound radiation at audio frequencies* (Springer Science & Business Media, 2013).

⁵ D. J. Mead, *Passive vibration control* (John Wiley & Sons Inc, 1999).

⁶ J. Den Hartog and J. Ormondroyd, "Theory of the dynamic vibration absorber," *ASME J. Appl. Mech* **50**, 11–22 (1928).

⁷ M. P. Singh, S. Singh, and L. M. Moreschi, "Tuned mass dampers for response control of torsional buildings," *Earthquake engineering & structural dynamics* **31**, 749–769 (2002).

⁸ L. Zuo and S. A. Nayfeh, "The two-degree-of-freedom tuned-mass damper for suppression of single-mode vibration under random and harmonic excitation," *Journal of vibration and acoustics* **128**, 56–65 (2006).

⁹ S.-M. Kim, S. Wang, and M. J. Brennan, "Dynamic analysis and optimal design of a passive and an active piezo-electrical dynamic vibration absorber," *Journal of sound and vibration* **330**, 603–614 (2011).

¹⁰ M. D. Rao, "Recent applications of viscoelastic damping for noise control in automobiles and commercial airplanes," *Journal of Sound and Vibration* **262**, 457–474 (2003).

¹¹ M. Khun, H. Lee, and S. Lim, "Structural intensity in plates with multiple discrete and distributed spring–dashpot systems," *Journal of Sound and Vibration* **276**, 627–648 (2004).

¹² M. N. Hadi and Y. Arfiadi, "Optimum design of absorber for mdof structures," *Journal of Structural Engineering* **124**, 1272–1280 (1998).

¹³ M. B. Ozer and T. J. Royston, "Extending den hartogs vibration absorber technique to multi-degree-of-freedom systems," *Journal of Vibration and Acoustics* **127**, 341–350 (2005).

¹⁴ J. Zapfe and G. Lesieutre, "Broadband vibration damping using highly distributed tuned mass absorbers," *AIAA journal* **35**, 753–755 (1997).

¹⁵ R. L. Harne and C. R. Fuller, "Modeling of a passive distributed vibration control device using a superposition technique," *Journal of Sound and Vibration* **331**, 1859–1869 (2012).

¹⁶ R. Harne, "On the linear elastic, isotropic modeling of poroelastic distributed vibration absorbers at low frequencies," *Journal of Sound and Vibration* **332**, 3646–3654 (2013).

- ¹⁷ C. Sun, S. Nagarajiah, and A. Dick, "Experimental investigation of vibration attenuation using nonlinear tuned mass damper and pendulum tuned mass damper in parallel," *Nonlinear Dynamics* **78**, 2699–2715 (2014).
- ¹⁸ Z. Yang, J. Mei, M. Yang, N. Chan, and P. Sheng, "Membrane-type acoustic metamaterial with negative dynamic mass," *Physical Review Letters* **101**, 204301 (2008).
- ¹⁹ J. Mei, G. Ma, M. Yang, Z. Yang, W. Wen, and P. Sheng, "Dark acoustic metamaterials as super absorbers for low-frequency sound," *Nature communications* **3**, 756 (2012).
- ²⁰ G. Ma, M. Yang, S. Xiao, Z. Yang, and P. Sheng, "Acoustic metasurface with hybrid resonances," *Nature Materials* **13**, 873–878 (2014).
- ²¹ M. Yang, G. Ma, Y. Wu, Z. Yang, and P. Sheng, "Homogenization scheme for acoustic metamaterials," *Physical Review B* **89**, 064309 (2014).
- ²² Songwen Xiao, Guancong Ma, Yong Li, Zhiyu Yang, and Ping Sheng, *Appl. Phys. Lett.* **106**, 091904 (2015).
- ²³ Min Yang, Chong Meng, Caixing Fu, Yong Li, Zhiyu Yang, and Ping Sheng, *Appl. Phys. Lett.* **107**, 104104 (2015).